

Langevin description of fission of hot metallic clusters

P. Fröbrich^a and A. Ecker

Hahn-Meitner-Institut Berlin, Glienicker Straße, 14109 Berlin, Germany

Received: 10 March 1998 / Revised: 5 June 1998 / Accepted: 17 June 1998

Abstract. A dynamical model of fission of hot charged metallic clusters on the basis of Langevin equations is proposed, where the viscosity is taken from experimental data for the bulk. As an example the process $\text{Na}_{18}^{2+} \rightarrow \text{Na}_9^+ + \text{Na}_9^+$ is considered. Decay rates calculated with the full Langevin equations are compared with those of the overdamped limit, which turns out to be a good approximation. Comparison is also made with the Bohr-Wheeler rate, the quasi-stationary Kramers rate, and a rate derived from a mean first passage time approach. A fission delay is predicted which is two orders of magnitude larger than in a calculation without dissipation. This is an order of magnitude larger than the corresponding effect in nuclear fission, where in contrast to the cluster case the fission delay due to friction is well established experimentally. A comparison is also made with the competing decay channels $\text{Na}_{18}^{2+} \rightarrow \text{Na}_{15}^+ + \text{Na}_3^+$, $\text{Na}_{18}^{2+} \rightarrow \text{Na}_{17}^+ + \text{Na}^+$, and $\text{Na}_{18}^{2+} \rightarrow \text{Na}_{17}^{2+} + \text{Na}$, which are treated as evaporation processes.

PACS. 36.40.Qv Stability and fragmentation of clusters

1 Introduction

The viscosity of nuclear matter considerably slows down the fission process of hot nuclei compared to the case without dissipation, see *e.g.* the review articles [1, 2]. The main experimental indicators for slow nuclear fission are the pre-scission neutron and γ multiplicities, *i.e.* the number of neutrons and giant dipole γ quanta, respectively, emitted per fission event prior to scission. No such experimental indicator for a delayed fission of metallic clusters exists up to now. Mass symmetric fission of metallic clusters has not even been identified experimentally; metallic clusters preferentially undergo asymmetric fission.

The different behaviour of nuclei and clusters can be understood on the basis of a liquid drop model which has been not only established for nuclei but also for clusters, *e.g.* [3]. Fission is controlled by the competition between the repulsive Coulomb interaction and the surface tension. Whereas nuclei are homogeneously charged, metallic clusters are surface charged. Calculating the driving forces with respect to the asymmetry degree of freedom in the liquid drop model explains why heavy nuclei prefer symmetric and metallic clusters strongly asymmetric fission. For a detailed discussion of this point see references [4, 5]. Experimentally it is established that the preferred decay channel of multiply charged alkali metal clusters below the so-called appearance size is a light singly charged (often a trimer) particle and the corresponding multiply charged heavy residual cluster, and not symmetric

fragmentation. This might be interpreted as very asymmetric fission. However, the process looks more like the evaporation of a light charged particle, which in nuclear physics would correspond to the evaporation of a proton or an α particle. Therefore it has been proposed in references [6–8] to treat the decay of hot clusters, not only for the emitted neutral monomers but also for the emitted light charged particles, on the basis of the Weisskopf [9] evaporation model appropriately modified for the application to clusters. By equating the decay rates for neutral monomer and charged particle emission the critical (appearance) sizes of alkali and alkaline earth metals produced at high temperatures have been calculated and compared with experimental data [10].

For a collective motion like fission into symmetric fragments an evaporation model is not adequate. One still may try a statistical model like that of Bohr and Wheeler [11] which was developed for nuclear fission. If, however, dynamics (not only the driving force but also viscosity) plays a role in the collective fission degree of freedom one might apply the quasi-stationary Kramers model [12] (based on a stationary solution of a Fokker-Planck equation) or alternatively, in order to have a completely dynamical description, one might solve the corresponding Langevin equations.

Symmetric fission of metallic clusters has been calculated on the basis of microscopic models, *e.g.* in references [13, 14]. But only in reference [14], where the fission process $\text{Na}_{18}^{2+} \rightarrow \text{Na}_9^+ + \text{Na}_9^+$ is treated, also the competing channel $\text{Na}_{18}^{2+} \rightarrow \text{Na}_{15}^+ + \text{Na}_3^+$ is investigated. It is found in this particular case that the barrier height for symmetric

^a also Fachbereich Physik, Freie Universität Berlin.
e-mail: froebrich@hmi.de

fission (note that the fission products Na_9^+ have closed shells) is comparable with the barrier height for the emission of a charged trimer. For energetic reasons the fission process, therefore, might well compete with the evaporation process. However, if viscosity plays a role the fission process should be suppressed as in the nuclear case. In reference [15] we have estimated the effect of viscosity on the fission rates of clusters by applying the quasi-stationary Kramers limit using the potential of reference [14] and the measured viscosity coefficient of the bulk [16]. It was predicted that the fission delay of clusters due to viscosity should be even an order of magnitude larger than the corresponding effect in the fission of hot nuclei. For a possible experiment on the decay of Na_{18}^{2+} this would have as consequence that symmetric fission is expected to be suppressed and the emission of charged trimers should dominate although the barrier heights of both processes are of about equal size.

In the present paper we improve the previous estimates by solving Langevin equations based on the one-dimensional (in terms of the fission coordinate q) potential of reference [14] for a dynamical calculation of the fission rate as a function of time, thus going beyond the quasi-stationary limit of Kramers. A treatment of fission of clusters with Langevin equations was also proposed by Rubchenya [17]. We compare the results obtained with the full Langevin equations with those of a Langevin equation in the overdamped limit. We also make a comparison with rates obtained with the Bohr-Wheeler formula and the quasi-stationary Kramers limits, and with a fission rate derived from a mean first passage time approach.

2 The Langevin model

In Figure 1 we show the scenario for the fission process. Langevin trajectories start at the position of the ground state q_{gs} of the fission potential $V(q)$, which is shown as a function of the fission coordinate q defined as the distance between the centers of mass between the fission fragments. The potential is normalised to $V(q_{gs}) = 0$. The initial momenta p are sampled from a thermal distribution with an initial temperature determined by the initial excitation energy of the system, $E_i^* = E_{tot} = (3n - 6)k_B T$. The total energy is subdivided into a kinetic energy E_{kin} , the potential energy $V(q)$, and the intrinsic excitation energy E^* , $E_{tot} = E_{kin} + V(q) + E^*$. The trajectories run over the saddle point with a barrier height B_f at q_{sd} and leave the potential at the scission point q_{sc} . The trajectories can also be reflected from the inner well before leaving the potential (see Fig. 3 for an example).

The trajectories are determined by solving the system of Langevin equations which in order to be suitable for numerical simulation are given in discretized form

$$\begin{aligned} q_{n+1} &= q_n + \left(\frac{p}{M}\right)_n \tau \\ p_{n+1} &= p_n - \left(\frac{dV(q)}{dq} + \eta \frac{p}{M}\right)_n \tau + \sqrt{(\eta T)_n} \tau w(t_n). \end{aligned} \quad (1)$$

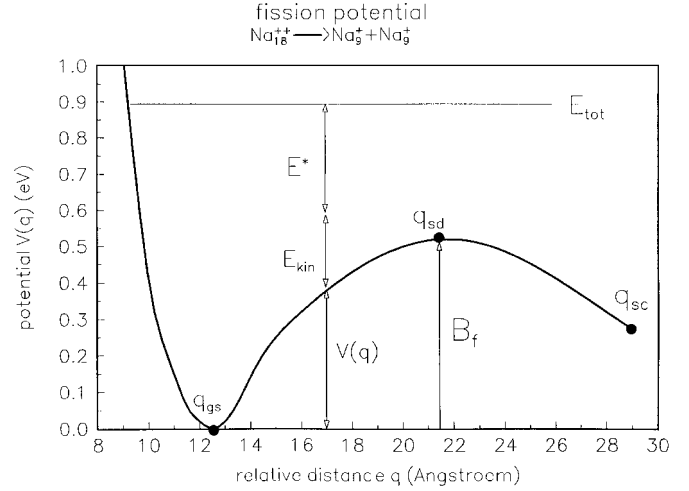


Fig. 1. The fission potential $V(q)$ for $\text{Na}_{18}^{2+} \rightarrow \text{Na}_9^+ + \text{Na}_9^+$. Indicated are the ground-state (q_{gs}), saddle-point (q_{sd}), and scission-point (q_{sc}) positions, and the fission barrier height B_f . The total energy is decomposed into the potential, kinetic, and excitation energy, $E_{tot} = V(q) + E_{kin} + E^*$.

Here τ is the time step used in the numerical simulations; in the case of clusters $\tau = 3 \times 10^{-15}$ s is used. Consistent with a previous publication [15] we restrict ourselves to the quadrupole mode of the hydrodynamical model, see *e.g.*

[18], *i.e.* we use for the inertia $M = \frac{3}{10} M_0 R_0^2$, where M_0 is the mass of the cluster, and for the viscosity coefficient $\eta = 4\pi R_0^3 \mu$, where R_0 is the radius of the cluster and μ the viscosity coefficient of the bulk. T is the temperature. The quantity $w(t_n)$ is a Gaussian random variable with mean value zero and, assuming Markovian friction, a δ -correlated variance

$$\begin{aligned} \langle w(t_n) \rangle &= 0 \\ \langle w(t_n) w(t_{n'}) \rangle &= 2\delta_{nn'}. \end{aligned} \quad (2)$$

In the overdamped case the relative motion is very slow due to a strong friction. One obtains the relevant equation for this case by dividing the second of equations (1) by the friction coefficient η , neglecting the term $(p_{n+1} - p_n)/\eta$, and solving for $q_{n+1} - q_n$, introducing the reduced friction coefficient $\beta = \eta/M$ (this is common practice in the nuclear physics literature)

$$q_{n+1} = q_n - \left(\frac{1}{\beta M} \frac{dV(q)}{dq}\right)_n \tau + \sqrt{\left(\frac{T}{\beta M}\right)_n} \tau w(t_n). \quad (3)$$

This equation corresponds to the Smoluchowski equation when transformed into a partial differential equation. Note that in the overdamped limit the equation does *not* depend on the inertia parameter, as this drops out because $\beta = \eta/M$. This means that, if the overdamped limit turns out to be a good approximation (and this will be the case for the fission of clusters), the inertia parameter is of no importance.

A time-dependent fission rate will then be calculated by sampling the number of trajectories N_i which have

fissioned in the time bin i

$$R(t) = \frac{1}{N_{tot} - N_f(t)} \frac{dN_f(t)}{dt}$$

$$\rightarrow R_i = \frac{1}{N_{tot} - \sum_{j=1}^i N_j} \frac{N_i}{\Delta t}. \quad (4)$$

Here N_{tot} are the total number of trajectories, $N_f(t)$ are the number of trajectories that have fissioned at the time t , and Δt is the width of the time bin.

In the limit of large times the Langevin calculations should approach the quasi-stationary limit of Kramers [12] if the latter is a good approximation. This requires that the behaviour of the system is solely characterized by its properties at the ground state and saddle, because the Kramers rate formulas express this feature.

The Kramers decay rate reads [12]

$$R^{Kram} = \frac{\hbar\omega_{gs} \omega_K}{2\pi\hbar \omega_{sd}} \exp\left(-\frac{B_f}{k_B T}\right). \quad (5)$$

Here ω_K is the Kramers frequency, $\omega_K = \sqrt{(\omega_{sd}^2 + \beta^2/4)} - \beta/2$, and $\omega_{sd} = \sqrt{(V''_{sd}/M_{sd})}$ and $\omega_{gs} = \sqrt{(V''_{gs}/M_{gs})}$ are the frequencies at the saddle and at the minimum of the fission potential given in terms of the curvatures $V''_{sd(gs)}$ and inertias $M_{sd(gs)}$ at the corresponding positions.

In the overdamped case ($\beta/(2\omega_{sd}) \gg 1$) the Kramers rate reduces to

$$R^{oKram} = \frac{\hbar\omega_{gs} \omega_{sd}}{2\pi\hbar \beta} \exp\left(-\frac{B_f}{k_B T}\right), \quad (6)$$

which is obtained by expanding the square root in ω_K .

For comparison we give also the Bohr-Wheeler decay rate [11] which, using the Einstein level density of a cluster of size n , has the form [15]

$$R_n^{BW} = \frac{1}{2\pi\hbar\rho_n(E)} \int_0^{E-B_f} d\epsilon \rho(E - B_f - \epsilon)$$

$$= \frac{k_B T}{2\pi\hbar} \left(1 - \frac{B_f}{(3n-6)k_B T}\right)^{3n-6}. \quad (7)$$

For large clusters ($(3n-6) \rightarrow \infty$) this formula goes over into the more familiar (for nuclei) expression

$$R_{n \rightarrow \infty}^{BW} = \frac{k_B T}{2\pi\hbar} \exp\left(-\frac{B_f}{k_B T}\right), \quad (8)$$

where we have used $\lim_{m \rightarrow \infty} (1 - x/m)^m = \exp(-x)$.

In the case without friction often the Arrhenius decay rate is applied, with the ‘‘attempt frequency’’ ω_{gs} as prefactor

$$R^{Arrh} = \frac{\hbar\omega_{gs}}{2\pi\hbar} \exp\left(-\frac{B_f}{k_B T}\right). \quad (9)$$

In nuclear fission sometimes also the Kramers modified Bohr-Wheeler expression

$$R^{KBW} = R_n^{BW} \frac{\omega_K \hbar\omega_{gs}}{\omega_{sd} k_B T} \quad (10)$$

is used [19], in order to correct approximately for viscosity effects. This reads in the overdamped limit

$$R^{oKBW} = R_n^{BW} \frac{\omega_{sd} \hbar\omega_{gs}}{\beta k_B T}. \quad (11)$$

These analytical expressions have been used in reference [15] in order to estimate the reduction of the fission rate of clusters due to viscosity effects.

In the present paper we compare the Langevin results also with a rate formula [20] which is valid in the overdamped case and is more accurate than Kramers limit. An approximation to this rate formula was applied extensively in nuclear fission [2] in cases where the Kramers limit is not a good approximation (*e.g.* for nuclei where the scission point is not far away from the saddle point). The exact formula is derived from a mean first passage time (MFPT) approach [20] and reads

$$R^{MFPT} = \frac{k_B T}{\beta M} \left(\int_{q_{gs}}^{q_{sc}} dx e^{V(x)/k_B T} \right. \\ \left. \times \int_{q_{ref}}^x dy e^{-V(y)/k_B T} \right)^{-1}. \quad (12)$$

This formula is based on the assumption that the inverse of a mean first passage time can be interpreted as a rate for the decay process. It should be more accurate than the limit of Kramers because it integrates over the whole range of the potential, whereas in the limit of Kramers only quadratic expansions of the potential at the ground state and saddle point enter. An approximation to equation (12) was used in reference [2] and is obtained by making expansions up to quadratic order in the inner integral around the ground-state position q_{gs} and in the outer integral around the saddle-point position and extending the lower limit of the inner integration to minus infinity ($q_{ref} \rightarrow -\infty$), the upper limit to infinity ($x \rightarrow \infty$), and setting in the outer integral $q_{gs} \rightarrow -\infty$. This results in

$$R_{appr}^{MFPT} = \frac{\omega_{gs}\omega_{sd}}{2\pi\beta} \exp\left(-\frac{B_f}{k_B T}\right) \\ \times \frac{2}{1 + \operatorname{erf}[(q_{sc} - q_{sd})\sqrt{(V''_{sd}/(2k_B T))}]}, \quad (13)$$

where $\operatorname{erf}(x) = (2/\sqrt{\pi}) \int_0^x dt \exp(-t^2)$ is the error function. In this formula the influence of the scission point position q_{sc} enters, which does not appear in the Kramers formula. If the scission point is far away from the saddle point the error function goes to unity and one recovers Kramers result. If the scission point coincides with the saddle point the error function is zero, which leads to an enhancement by a factor of two as compared to the situation where the scission point is far away from the saddle point. Below we will show how the position of the scission point influences the decay rate.

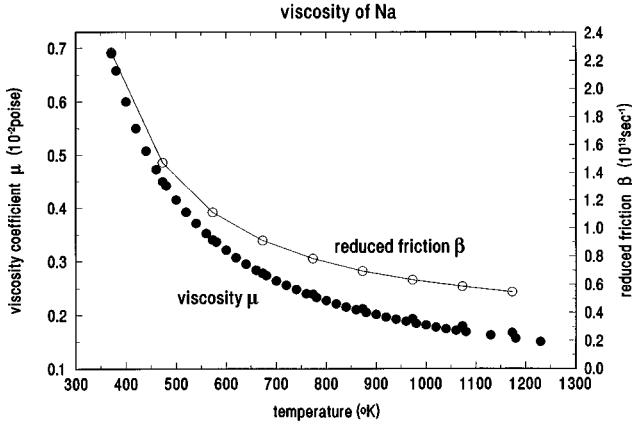


Fig. 2. The experimental [16] bulk viscosity $\mu[10^{-2}$ poise] and the reduced friction parameter $\beta[10^{13} \text{ s}^{-1}]$ for Na_{18}^{2+} are plotted as functions of the temperature.

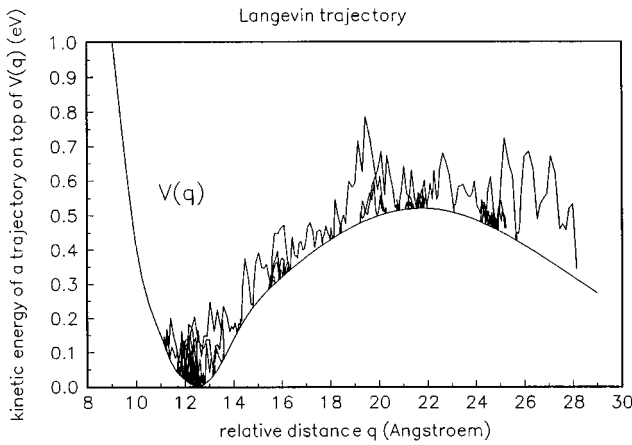


Fig. 3. The kinetic energy of a Langevin trajectory, which starts at the ground-state position, moves over the saddle, and leaves the potential at the scission point, is plotted on top of the potential $V(q)$.

3 Calculated fission rates

In the following we first present results of calculations for the fission decay rates obtained from the full Langevin equations, equation (1), and with the overdamped Langevin equation, equation (3), for the process $\text{Na}_{18}^{2+} \rightarrow \text{Na}_9^+ + \text{Na}_9^+$ at the temperatures 1073 K, 773 K, and 673 K. As viscosity coefficient we use the measured bulk value $\mu(T)$ of liquid Na [16], because viscosity coefficients for finite systems are not available. In Figure 2 we plot the temperature dependence of $\mu(T)$ and of the reduced friction parameter $\beta(T) = \eta/M = 4\pi R_0^{1/3} \mu(T)/(3/10M_0)$ for Na_{18}^{2+} .

In Figure 3 we show as an example a particular Langevin trajectory which starts at the minimum of the potential q_{gs} with a momentum sampled from a thermal distribution. Plotted is the kinetic energy plus the potential $V(q)$. The trajectory moves over the maximum of the potential at the position q_{sd} , and ends at the scission

point q_{sc} . As potential we use a smooth curve fitted to the potential shown in Figure 2 of reference [14].

On the left-hand side of Figure 4 we display histograms of the time-dependent fission rates for $T = 1073 \text{ K}$, 773 K , 673 K for the full Langevin equations, equation (1). After a delay time t_d (which increases slightly with decreasing temperature) the decay rates approach a stationary limit, *i.e.* they do not change with time any more. For large times these rates should approach the quasi-stationary limit of Kramers, equation (5), if the latter is a good approximation. The extent to which this is the case can be read off from the figure in which we have entered the result of the Kramers formula. For comparison we also display the overdamped quasi-stationary Kramers result, equation (6), which in the considered cases is not much larger than the full Kramers result.

On the right-hand side of Figure 4 we plot the Langevin rates for the overdamped situation, using equation (3). Comparing with the full Langevin rates one observes that the overdamped Langevin rates are larger than the full Langevin rates by about the same amount as the corresponding quasistationary Kramers limits. We also compare with the rate of the mean first passage time approach, equation (12), which can be derived in closed form only in the overdamped limit. It is closer to the overdamped Langevin approach (exact within the statistical errors) than the overdamped Kramers limit. This is due to the fact that it is expected to be more accurate than the limit of Kramers because integrations in equation (12) are performed over the whole range of the potential, whereas the Kramers limit uses only quadratic expansions of the potential around the ground state and saddle point positions.

One learns from the figures that the fission of clusters follows very closely an overdamped motion; the rates of the overdamped limit are less than 10% larger than those of the full calculations. The calculations also show that if one is only interested in the fission rates the Kramers limit is a good approximation, and it is not necessary to perform time-consuming Langevin calculations (in particular at low temperatures when only a small fraction of the trajectories undergoes fission so that one has to run many trajectories in order to obtain a reasonable statistics).

The precise values for the fission rates as functions of the temperature obtained with the various approximate analytical formulas, equations (5) to (13), can be read from Table 1. These rates are also plotted in Figure 5.

It is interesting to make a comparison of Kramers result with the MFPT approach for cases where the scission point is moved closer to the saddle point (this occurs in the case of lighter fissioning nuclei but *not* for the cluster example discussed above). The corresponding results, which show the influence of the position of the scission point on the rate, are shown in Figure 6. One observes that if the scission point is equal to the saddle point $q_{sc} = q_{sd}$ the rate calculated with the mean first passage time approach is twice the overdamped Kramers rate ($R_{appr}^{MFPT}/R_{Kram}^o = 2$), whereas R_{Kram}^o approaches R_{appr}^{MFPT} for $q_{sc} \gg q_{sd}$.

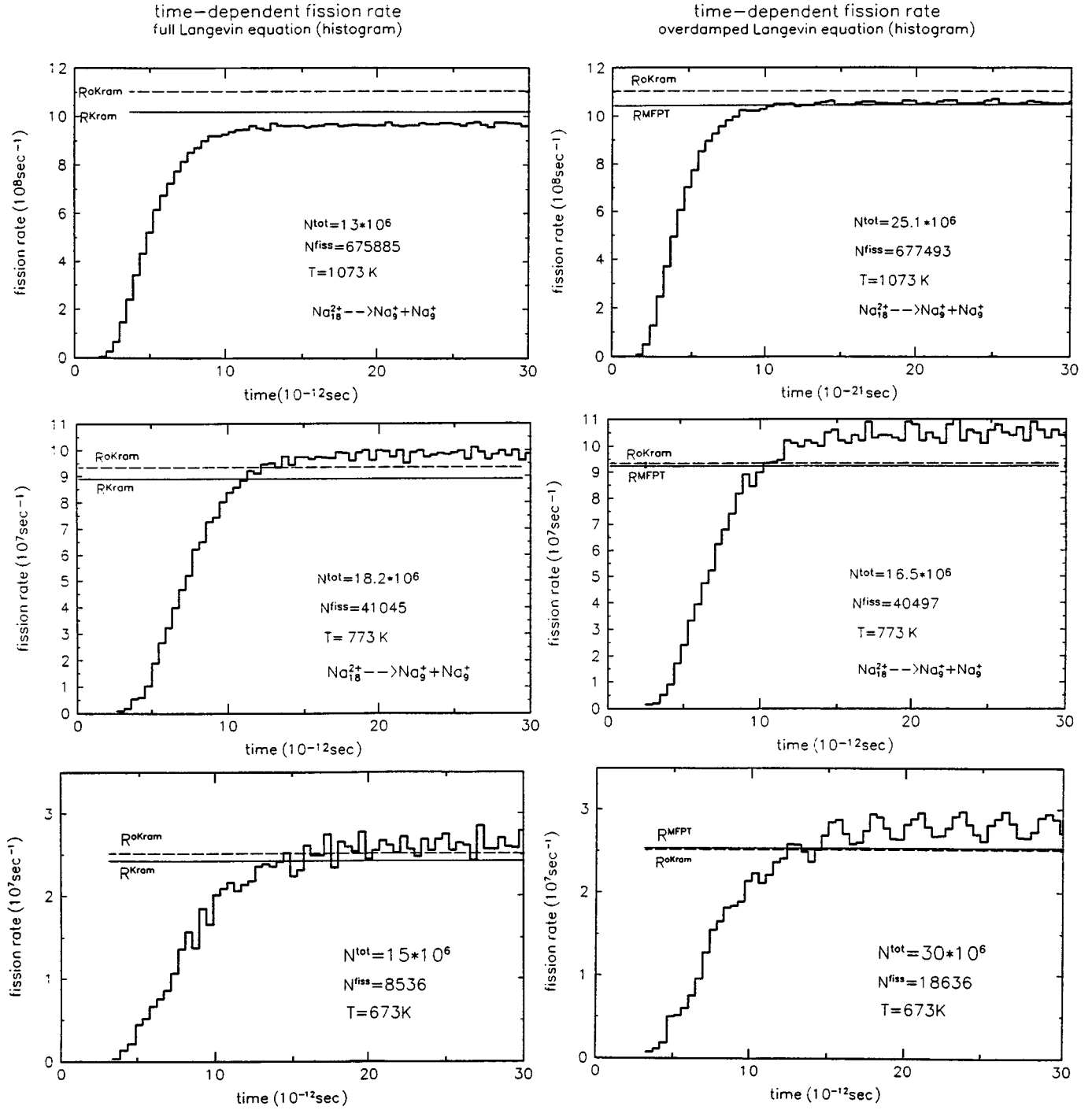


Fig. 4. Left-hand side: The time-dependent fission rates (histograms) calculated with the full Langevin equations are plotted as function of time for the temperatures $T = 1073$ K, 773 K, 673 K. N_{tot} is the total number and N_{fiss} the number of fissioning trajectories. For comparison the quasi-stationary Kramers rate R^{Kram} and the overdamped Kramers rate R^{oKram} are shown. Right-hand side: The same for the overdamped Langevin equation. A comparison is made with the overdamped Kramers rate R^{oKram} and the rate of the mean first passage time approach R^{MFPT} .

Table 1. Tabulated are the following fission rates as functions of the temperature.

T [° K]	R(BW)	R(BW,inf)	R(KBW)	R(oKBW)	R(Kram)	R(oKram)	R(Arrh)	R(aMFPT)	R(MFPT)
371	1.83×10^4	6.67×10^5	1.87×10^2	1.88×10^2	6.81×10^3	6.86×10^3	8.32×10^4	6.86×10^3	7.25×10^3
473	3.57×10^6	2.84×10^7	4.35×10^4	4.42×10^4	3.45×10^5	3.51×10^5	2.78×10^6	3.51×10^5	3.64×10^5
573	8.19×10^7	3.19×10^8	1.08×10^6	1.11×10^6	4.19×10^6	4.30×10^6	2.57×10^7	4.30×10^6	4.38×10^6
673	6.86×10^8	1.79×10^9	9.27×10^6	9.65×10^6	2.42×10^7	2.52×10^7	1.23×10^8	2.52×10^7	2.52×10^7
773	3.21×10^9	6.56×10^9	4.34×10^7	4.58×10^7	8.86×10^7	9.34×10^7	3.93×10^8	9.34×10^7	9.20×10^7
873	1.04×10^{10}	1.81×10^{10}	1.39×10^8	1.48×10^8	2.41×10^8	2.57×10^8	9.60×10^8	2.57×10^8	2.50×10^8
973	2.65×10^{10}	4.11×10^{10}	3.43×10^8	3.71×10^8	5.33×10^8	5.75×10^8	1.95×10^9	5.75×10^8	5.50×10^8
1073	5.64×10^{10}	8.07×10^{10}	7.08×10^8	7.73×10^8	1.01×10^9	1.11×10^9	3.48×10^9	1.11×10^9	1.04×10^9
1173	1.06×10^{11}	1.43×10^{11}	1.29×10^9	1.42×10^9	1.73×10^9	1.91×10^9	5.62×10^9	1.92×10^9	1.78×10^9

R(BW,inf): Bohr-Wheeler rate for large systems, equation (8). R(BW): Bohr-Wheeler rate for $n = 18$, equation (7). R(Arrh): Arrhenius rate, equation (9). R(Kram): Kramers rate, equation (5). R(oKram): overdamped Kramers rate, equation (6). R(aMFPT): approximate mean first passage time rate, equation (13). R(KBW): Kramers modified Bohr-Wheeler rate, equation (10). R(oKBW): overdamped Kramers modified Bohr-Wheeler rate, equation (11). R(MFPT): exact mean first passage time rate, equation (12).

The saddle-point and ground-state frequencies are slightly different from those used in reference [15]: $\omega_{sd} = 1.86 \times 10^{12} \text{ s}^{-1}$, $\omega_{gs} = 6.06 \times 10^{12} \text{ s}^{-1}$.

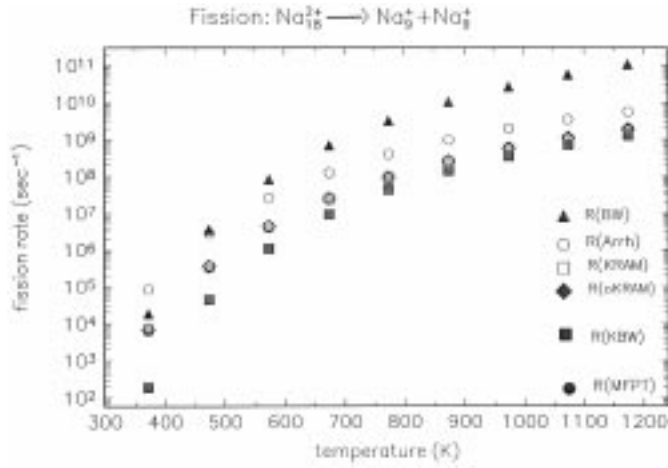


Fig. 5. Compared are quasi-stationary fission rates calculated with different expressions explained in the text: R(BW): Bohr-Wheeler rate for $n = 18$, equation (7); R(Arrh): Arrhenius rate, equation (9); R(Kram): Kramers rate, equation (5); R(oKram): overdamped Kramers rate, equation (6); R(KWB): Kramers modified Bohr-Wheeler rate, equation (10); R(MFPT): exact mean first passage time rate, equation (12).

4 Competing evaporation channels

In order to compare the fission decay with the competing evaporation channels: $\text{Na}_{18}^{++} \rightarrow \text{Na}_{17}^{++} + \text{Na}_1$, $\text{Na}_{18}^{++} \rightarrow \text{Na}_{17}^{+} + \text{Na}_1^{+}$, and $\text{Na}_{18}^{++} \rightarrow \text{Na}_{15}^{++} + \text{Na}_3^{+}$, we have calculated the corresponding decay rates with the evaporation model explained and applied in references [5, 8]. This comparison is made in Figure 7. Without taking viscosity into account the fission channel is predicted to be dominant; this is shown by the Bohr-Wheeler rate (R(BW), equation (7), solid triangles up). Taking viscosity into account by *e.g.* using the Kramers modified Bohr-Wheeler rate (R(KBW), equation (10), solid squares) the fission rate is suppressed by two orders of magnitude. For not too high temperature the weakest evaporation channel is the emission of a neutral monomer (Na_1 , open circles),

Dependence of the fission rate on the position of the scission point q_{sc}

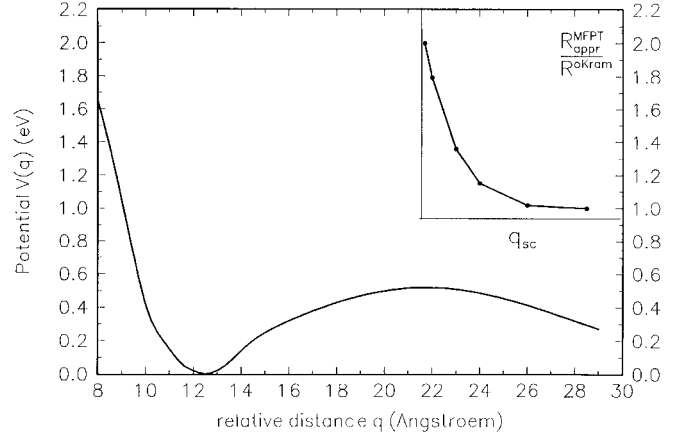


Fig. 6. The fission potential $V(q)$ as function of the distance between the centers of mass of the fission fragments. The inset shows the ratio of the fission rates $R_{appr}^{MFPT}/R^{oKram}$ as function of the scission point position q_{sc} ; the latter is chosen at different positions of the potential $V(q)$ with values on the abscissa of the outer frame. For $q_{sc} = q_{sd} = 21.4 \text{ \AA}$ one finds $R_{appr}^{MFPT}/R^{oKram} = 2$; for $q_{sc} \gg q_{sd}$ the rate R^{oKram} approaches R_{appr}^{MFPT} , *i.e.* $R_{appr}^{MFPT}/R^{oKram} = 1$.

whereas the Coulomb repulsion enhances the evaporation of the charged monomer (Na_1^{+} , open squares). The emission of a charged trimer is even stronger (Na_3^{+} , open triangles down). These calculations suggest that the evaporation of a charged trimer should be the dominant process in the decay of Na_{18}^{++} if the probability of fission is reduced by the action of viscosity. The reason that the fission channel, even after including the viscosity, remains dominant over the monomer emission channel is connected with the fact that in the present case (decay of Na_{18}^{++}) the shell structure (magic numbers of the fission fragments) is particularly pronounced. With less pronounced shell effects the driving potential for the asymmetry degree of

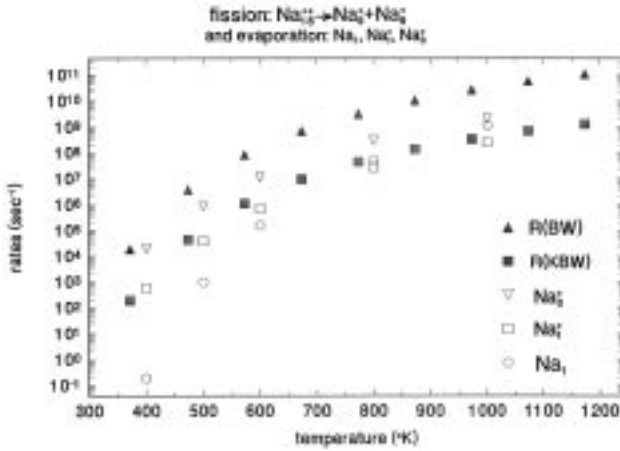


Fig. 7. $\text{Na}_{18}^{2+} \rightarrow \text{Na}_9^+ + \text{Na}_9^+$ neglecting viscosity (R(BW), equation (7), solid triangles up), and with taking viscosity into account (R(KBW), equation (10), solid squares). For comparison evaporation rates for the processes: $\text{Na}_{18}^{2+} \rightarrow \text{Na}_{15}^+ + \text{Na}_3^+$ (open triangles down), $\text{Na}_{18}^{2+} \rightarrow \text{Na}_{17}^+ + \text{Na}_1^+$ (open squares), and $\text{Na}_{18}^{2+} \rightarrow \text{Na}_{17}^{2+} + \text{Na}_1$ (open circles) are shown.

freedom prefers the emission of monomers over a symmetric fragmentation, as *e.g.* discussed in references [4, 5].

5 Conclusions

The Langevin calculations confirm on a dynamical level the result of reference [15], namely that if viscosity plays a role in cluster fission, the fission decay rates of alkali clusters (more precisely for Na_{18}^{2+}) are suppressed by two orders of magnitude as compared to the case without dissipation. This predicts an effect which is an order of magnitude larger than the corresponding experimentally observed effect in nuclear fission. It would have the consequence that in an experiment on the decay of Na_{18}^{2+} the emission of Na_3^+ should be dominant over symmetric fission, even if the corresponding barriers are of comparable height. It is confirmed that if the bulk viscosity is a reasonable order of magnitude estimate for finite clusters, the motion in the fission degree of freedom is overdamped to a good approximation. If one is interested only in fission rates (and competing channels do not play a role) it is not necessary to perform Langevin calculations because estimates with the Kramers quasi-stationary rates give results which deviate less than 10% from the more exact Langevin results.

It is necessary to perform dynamical calculations when dealing with the dynamical coupling of the different decay modes (fission, evaporation of charged and neutral light cluster particles, radiation), because the different channels would influence each other during the decay process. In particular this is true if the assumptions of a statistical model are not fulfilled. An alternative would be the description of cluster fragmentation by molecular dynamics, which not only allows the treatment of all degrees of freedom explicitly, but treats also the various fragmentation channels. A representative paper in this connection

is reference [21], and references therein, which also makes a comparison with theoretical statistical models. A model for the competing channels was also found to be necessary for the dynamical description of fission of hot nuclei, where a large variety of data exists [1, 2]. Analogous experiments on the decay of hot clusters would be of great interest. If they are done it would be worthwhile to work out the corresponding theory in more detail. The development hopefully will be faster than in nuclear fission where a statistical model [11] turned out to be sufficient for forty years before experiments (concerning pre-scission neutron multiplicities) in the eighties enforced a detailed dynamical theoretical description (for reviews, see Refs. [1, 2]).

We are indebted to P. Jensen and R. Lipperheide for a careful reading of the manuscript.

References

1. D. Hilscher, H. Rossner, *Ann. Phys. Fr.* **17**, 471 (1992).
2. P. Fröbrich, I.I. Gontchar, *Physics Rep.* **292**, 131 (1998).
3. W.A. Saunders, *Phys. Rev. Lett.* **64**, 3046 (1990) and *Phys. Rev. A* **46**, 7028 (1992); C. Bréchnignac *et al.*, *Phys. Rev. B* **44**, 11368 (1991).
4. U. Näher, S. Bjørnholm, S. Frauendorf, F. Garcias, C. Guet, *Phys. Rep.* **285**, 245 (1997).
5. P. Fröbrich, *J. Phys. G* **23**, 1439 (1997).
6. P. Fröbrich, *Phys. Lett. A* **202**, 99 (1995).
7. P. Fröbrich, *Z. Phys. D* **40**, 198 (1997).
8. P. Fröbrich, *Ann. Physik* **6**, 403 (1997).
9. V. Weisskopf, *Phys. Rev.* **52**, 295 (1937).
10. P. Fröbrich, *Proc. Int. Symp., Similarities and Differences between Atomic-Nuclei and -Clusters*, Tsukuba, Japan, July 1-4, 1997, edited by Abe, Arai, Lee, Yabana, (The American Institute of Physics 1-56396-714-6, 1998), p. 139; *Proc. Int. Symp., Atomic Nuclei and Metallic Clusters*, Prague, Czech. Rep., Sept. 1-5, *Czech. J. Phys.* **48**, 799 (1998).
11. N. Bohr, J.A. Wheeler, *Phys. Rev.* **56**, 426 (1939).
12. H.A. Kramers, *Physica* **7**, 284 (1940).
13. C. Yannouleas, U. Landman, *Nato ASI Series E: Applied Sciences vol. 313*, edited by T.P. Martin (Kluwer Academic Publishers, The Netherlands, 1996), p. 121.
14. B. Montag, P.-G. Reinhard, *Phys. Rev. B* **52**, 16365 (1995), see also P.-G. Reinhard, F. Calvayrac, E. Suraud, *Z. Phys. D* **41**, 151 (1997).
15. P. Fröbrich, *Phys. Rev. B* **56**, 6450 (1997).
16. *CRC Handbook of Chemistry and Physics*, 49th edition, edited by R.C. Weast, pp. F-59, and 76th edition, edited by D.R. Lide, 1995-1996, pp. 6-261.
17. V.A. Rubchenya, *Lecture Notes in Physics* **404**, 98 (1992).
18. K. T. R. Davies, A.J. Sierk, J.R. Nix, *Phys. Rev. C* **13**, 2385 (1976).
19. N. D. Mavlitov, P. Fröbrich, I.I. Gontchar, *Z. Phys. A* **342**, 195 (1992).
20. L.A. Pontryagin, A. Andronov, A. Vitt, *Zh. Eksp. Teor. Fiz.* **3**, 165 (1933).
21. M.J. Lopez, J. Jellinek, *Phys. Rev. A* **50**, 1445 (1994).